Parallel electron beam excitation of surface plasmon polaritons in double layer graphene sheets

Gong Sen, Hu Min, Zhong Renbing, Chen Xiaoxing, Zhang Ping, Zhao Tao, and Liu Shenggang *

Cooperative Innovation Centre of THz Science, University of Electronic Science and Technology of China,Chengdu,610054, China

* Email: liusg@uestc.edu.cn

(Received November 30, 2015)

Abstract: In this paper, we present the parallel electron beam excitation of the surface plasmon polaritons (SPPs) in the double layer graphene sheets. The results of the theoretical analysis and numerical calculations show that the excited SPPs in the double layer graphene sheets have many characteristics and advantages compared to that in single layer graphene sheet. For the double layer graphene sheets, SPPs are spilt into two modes due to the coupling of SPPs, and the mode with higher frequency can be excited by parallel electron beam efficiently. The excited SPPs have higher operating frequencies and stronger field amplitudes than that in single layer graphene sheet, and the operating frequency can also be tuned by electron beam energy and chemical potential.

Keywords: Electron beam, Double layer graphene sheets, Surface plasmon polaritons.

doi: 10.11906/TST.170-178.2015.12.16

I. Introduction

Because of the exceptional properties [1-3] and great potential applications of graphene [4-8], it has become the most attractive research area in modern science and technology. Graphene-based plasmonics can play a versatile role for developing photonic and optoelectronic applications, such as ultrafast lasers, solar cells, optical modulators, photodetectors, and light devices [9]. One of the most interesting and important topics in graphene graphene-based plasmonics is the generation of THz radiation, for that the plasmon frequency of graphene lies in the 1-50 terahertz (*THz*) frequency regime [10], and the operating frequency of graphene surface plasmon polaritons (SPPs) can be tuned not only by the electron beam (e-beam) energy but also by the chemical potential [11]. It has been reported that graphene SPPs can be excited by parallel moving e-beam and transformed into THz radiation waves by the periodical dielectric substrates [11-13]. And it is also reported that the HEM mode ($TM_{mn}+TE_{mn}$) of graphene SPPs in cylindrical structures can be excited by cyclotron e-beam and transformed into tunable and coherent THz radiation [14]. These open new ways for room temperature, tunable and power enhanced THz radiation sources.

Graphene SPPs can also be excited by incident plane waves and e-beam. For incident plane wave excitation, special experimental arrangements have to be designed to provide conservation of the wave vector [15, 16] for the wave vector of graphene SPPs is larger than that of incident plane wave. Different from plane wave excitation, graphene SPPs can be excited by both perpendicularly and parallel moving e-beam directly [17-20].

In this paper, we present the parallel moving e-beam excitation of SPPs in double layer graphene sheets. The excited SPPs have higher operating frequency and larger amplitudes than that in single layer graphene. This paper is organized as below: the theoretical analysis is given in section II, the numerical calculation is presented in section III, and section IV is the conclusion.

II. Theoretical analysis

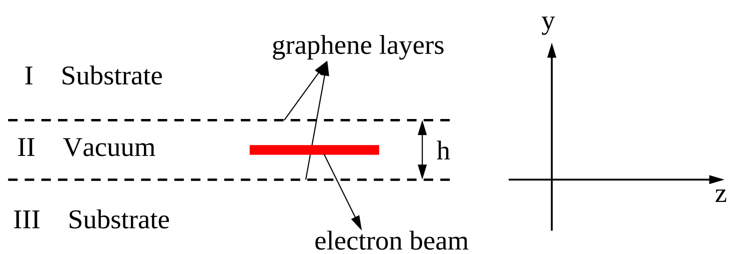

Fig. 1 The schematic of the double layer graphene sheets, the distance between the two graphene sheets is h.

The schematic of the e-beam excitation of SPPs in double layer graphene sheets is shown in figure 1. The two graphene sheets are covered on the two substrates, respectively, and the e-beam is moving parallel in the vacuum between the two substrates. In terahertz region, only the intraband conductivity dominates the process of graphene SPPs, and then the conductivity of graphene sheet is given as [11]:

$$\sigma = \sigma_{intra} = i\frac{e^2 k_B T}{\pi\hbar^2\left(\omega + i\tau^{-1}\right)}\left[\frac{\mu_C}{k_B T} + 2\ln\left(\exp\left(-\frac{\mu_C}{k_B T}\right)+1\right)\right] \tag{1}$$

where T is temperature, k_B is Boltzmann constant, τ is relaxation time, and μ_c is chemical potential. In this paper, values of $\mu_c = (0.15 \sim 0.35)\ eV$, $\tau = 0.5\ ps$, and $T = 300\ K$ are used for all numerical calculations.

This structure can be divided into three regions: region I and III are the substrates, and region II is the vacuum. Then the boundary conditions should be:

$$\begin{aligned} &E_z^{\ I}\Big|_{y=h} = E_z^{\ II}\Big|_{y=h} \qquad && -H_x^{\ I}\Big|_{y=h} + H_x^{\ II}\Big|_{y=h} = \sigma E_z^{\ I}\Big|_{y=h} \\ &E_z^{\ II}\Big|_{y=0} = E_z^{\ III}\Big|_{y=0} \qquad && -H_x^{\ II}\Big|_{y=0} + H_x^{\ III}\Big|_{y=0} = \sigma E_z^{\ III}\Big|_{y=0} \end{aligned} \tag{2}$$

The superscript I, II and III denote the regions of the fields. Based on the Maxwell's equations, and the boundary conditions in Eq. (2), the dispersion equation of the double layer graphene sheets is given as:

$$\frac{\left(+\dfrac{j\omega\varepsilon_0\varepsilon_1}{k_y^{\ I}} + \dfrac{j\omega\varepsilon_0\varepsilon_2}{k_y^{\ II}} - \sigma\right)}{\left(+\dfrac{j\omega\varepsilon_0\varepsilon_1}{k_y^{\ I}} - \dfrac{j\omega\varepsilon_0\varepsilon_2}{k_y^{\ II}} - \sigma\right)}\frac{e^{k_y^{\ II}h}}{e^{-k_y^{\ II}h}} = \frac{\left(-\dfrac{j\omega\varepsilon_0\varepsilon_2}{k_y^{\ II}} + \dfrac{j\omega\varepsilon_0\varepsilon_3}{k_y^{\ III}} - \sigma\right)}{\left(+\dfrac{j\omega\varepsilon_0\varepsilon_2}{k_y^{\ II}} + \dfrac{j\omega\varepsilon_0\varepsilon_3}{k_y^{\ III}} - \sigma\right)} \tag{3}$$

where ε_1, ε_2 and ε_3 is the relative permittivity of the three regions, respectively, and $k_y^{\ I} = \sqrt{k_z^{\ 2} - \varepsilon_1 k_0^{\ 2}}$, $k_y^{\ II} = \sqrt{k_z^{\ 2} - \varepsilon_2 k_0^{\ 2}}$, $k_y^{\ III} = \sqrt{k_z^{\ 2} - \varepsilon_3 k_0^{\ 2}}$, $k_0 = \omega / c$, c is the velocity of light in vacuum. When this structure is excited by parallel moving e-beam, there is $k_z = \omega / u_0$, where u_0 is the velocity of the e-beam.

Making use of the nonhomogeneous Helmholtz equation, the incidents waves of the parallel moving e-beam, $E_z^{\ i}$ and $H_x^{\ i}$, can be obtained [21], and then the boundary conditions of the excitation should be:

$$\begin{aligned} &E_z^{\ I}\Big|_{y=h} = E_z^{\ II}\Big|_{y=h} + E_z^{\ i}\Big|_{y=h} \qquad && -H_x^{\ I}\Big|_{y=h} + H_x^{\ II}\Big|_{y=h} + H_x^{\ i}\Big|_{y=h} = \sigma E_z^{\ I}\Big|_{y=h} \\ &E_z^{\ II}\Big|_{y=0} + E_z^{\ i}\Big|_{y=0} = E_z^{\ III}\Big|_{y=0} \qquad && -H_x^{\ II}\Big|_{y=0} - H_x^{\ i}\Big|_{y=0} + H_x^{\ III}\Big|_{y=0} = \sigma E_z^{\ III}\Big|_{y=0} \end{aligned} \tag{4}$$

Solving this equation set, the SPPs fields excited by parallel moving e-beam can be obtained.

III. Numerical calculations

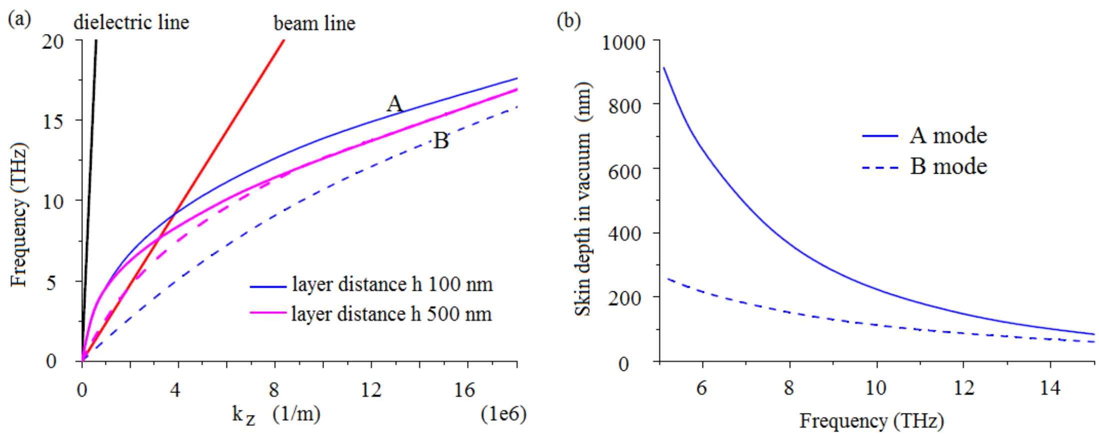

Fig. 2 (a) Dispersion curves of double layer graphene sheets with different layer distance h, $\varepsilon_1 = \varepsilon_3 = 2$, and $u_0 = 0.08c$, $\mu_c = 0.15\ eV$; (b) The skin depth in vacuum of SPPs for $h = 100\ nm$, $\varepsilon_1 = \varepsilon_3 = 2$, $\mu_c = 0.15\ eV$

The dispersion curve of SPPs in double layer graphene sheets is shown in figure.2 (a), and it can be seen that the graphene SPPs is split into two modes (A mode and B mode) due to the coupling between the excited SPPs on each graphene sheet. As shown in figure.2 (a), the frequency of A mode is higher than that of single layer graphene sheet at the same wave vector, and it is also higher when the layer distance is 100 *nm* than that when the layer distance is 500 *nm*. Different from A mode, the behavior of B mode is totally opposite to that of A mode. However, with the increase of the frequency, the dispersion curves of both A mode and B mode tend to be the same as that of the SPPs in single layer graphene sheet. Shown as the pink curves in figure.2 (a), when the layer distance is 500 *nm* and the frequency is larger than 11 *THz*, the dispersion curves of A mode and B mode merge into one curve, and this dispersion curve is similar as that of single layer graphene sheet.

The characteristics of the dispersion curves of SPPs in double layer graphene sheet are caused by the coupling of the excited SPPs on each graphene sheet. It can be seen from figure.2 (b) that the skin depth of the SPPs in double layer graphene sheet is about 1 micrometer. Accordingly, when the layer distance between the two graphene sheets is larger than 1 micrometer, the coupling of SPPs is very weak, so that the dispersion curves behave like that of the single layer graphene sheet. And it also can be seen from figure.2 (b) that the skin depth decreases with the increase of the frequency. So the SPPs coupling in the lower frequency region is much stronger than that in the higher frequency region. Accordingly, the spilt two modes merge into one mode when the SPPs frequency is very high.

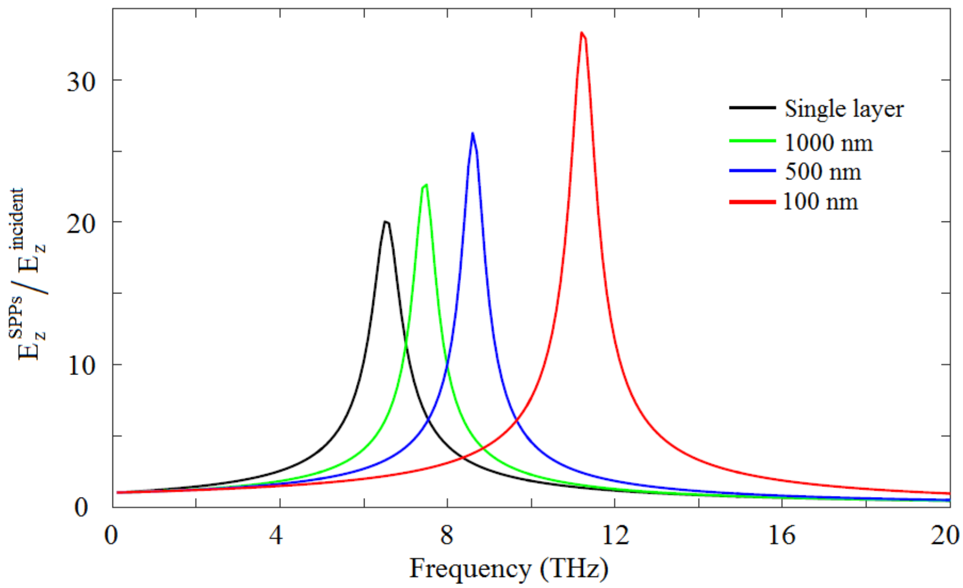

Fig. 3 The normalized amplitudes of the excited SPPs in double layer graphene sheet with different layer distance, $\varepsilon_1 = \varepsilon_3 = 1$, $u_0 = 0.08c$, $\mu_c = 0.15\ eV$.

Although there are two modes for the SPPs in double layer graphene sheets, the results of the numerical calculations show that the B mode is not easy to be excited, so we focus on the e-beam excitation of A mode. Figure.3 shows the dependence of the amplitudes of the excited SPPs in double layer graphene sheet on the layer distance, and the amplitudes of SPPs field are normalized by that of the incident waves generated by the parallel moving e-beam. It can be seen that when the layer distance is 100 *nm*, the excited SPPs get the largest field amplitude, which is up to 34. The field amplitudes decrease with the increase of the layer distance, and it gets the smallest value, 20, for the single layer graphene sheet. The operating frequency of the excited SPPs also decreases with the increase of the layer distance, and when the layer distance is 100 *nm*, it gets the highest frequency 11.5 *THz*, which is much higher than that for the single layer graphene sheet (6.5 *THz*) for the same e-beam energy. This is because the smaller layer distance means the stronger SPPs coupling, and returns a larger amplitude and higher operating frequency of the excited SPPs.

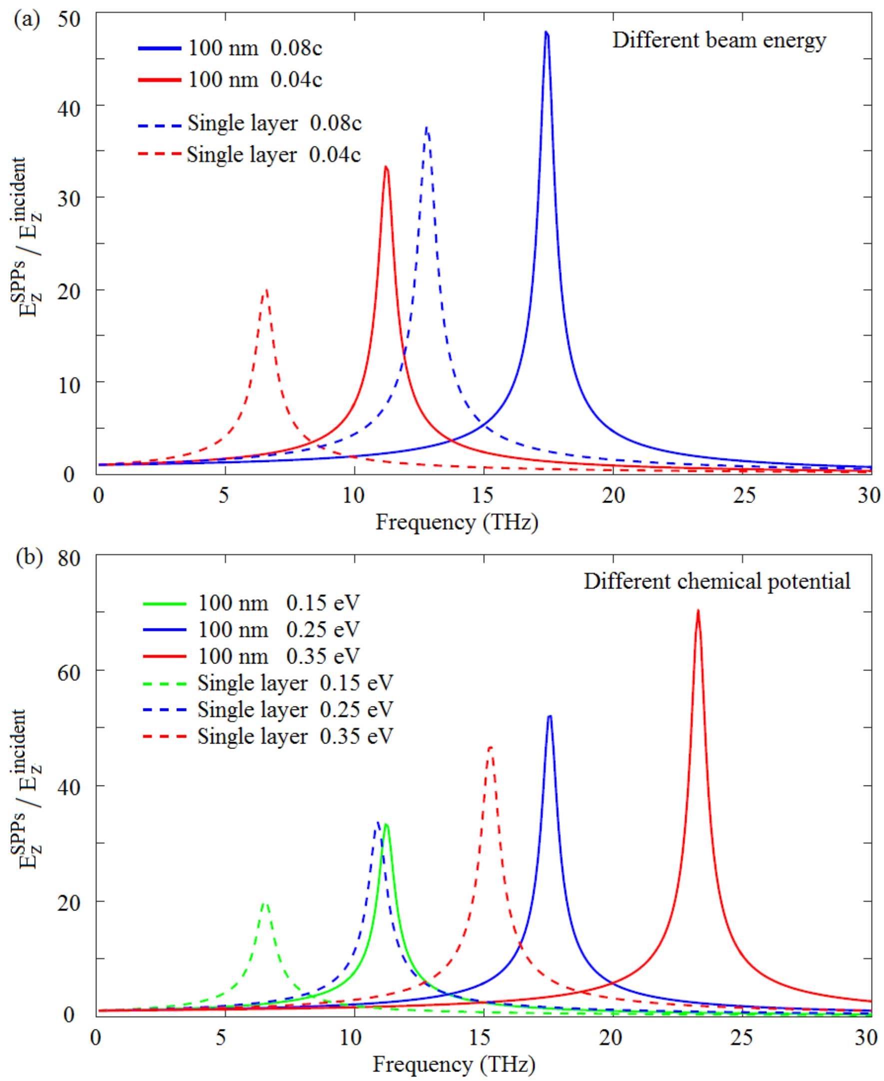

Fig. 4 The field spectrum of excited SPPs: (a) The excitation of SPPs in double layer graphene sheets with different e-beam energy, $\varepsilon_1 = \varepsilon_3 = 1$, $\mu_c = 0.15\, eV$; (b) The excitation of SPPs in double layer graphene sheets with different chemical potential, $\varepsilon_1 = \varepsilon_3 = 1$, $u_0 = 0.08c$.

The operating frequency of the excited SPPs in double layer graphene sheets can also be tuned by both the energy of the parallel moving e-beam and the chemical potential of the graphene sheet, as shown in figure.4 (a) and (b). It can be seen from figure.4 (a) and (b) that the operating frequency of the excited SPPs in the double layer graphene sheets with layer distance 100 *nm* increases with the increase of the e-beam energy or the chemical potential, and it can be tuned from 10.5 *THz* to 18 *THz* within the e-beam energy ranging from 0.04 *c* to 0.08 *c*, and from 11.5 *THz* to 24 *THz* within the chemical potential ranging from 0.15 *eV* to 0.35 *eV*. This is because the operating frequency of the excited SPPs is determined by the intersection point of the dispersion curve and the beam line for the parallel e-beam excitation [19]. Figure.4 (a) and (b) also show that the coupling of the excited SPPs provides larger field amplitude and higher operating frequency for the double layer graphene sheets than the single layer graphene sheet.

IV. Conclusion

In this paper, we present the parallel e-beam excitation of the SPPs in the double layer graphene sheets. The results of the theoretical analysis and numerical calculations show that the excited SPPs in the double layer graphene sheets have many characteristics and advantages compared to that in single layer graphene sheet. For the double layer graphene sheets, SPPs are spilt into two modes due to the coupling of SPPs, and the mode with higher frequency can be excited by parallel e-beam efficiently. The excited SPPs in double layer graphene sheets have higher operating frequencies and larger field amplitudes than that in single layer graphene sheet, and the operating frequency can also be tuned by e-beam energy and chemical potential.

Acknowledgement

This work is supported by the National Basic Research Program under grants No.2014CB339801, the Natural Science Foundation of China under Grant No. 61231005, No. 11305030 and No. 612111076, and National Hightech Research and Development Project under contract No. 2011AA010204

References

1. Neto A H C, Guinea F, Peres N M R, et al. "The electronic properties of graphene[J]". *Reviews of modern physics*, 81(1): 109 (2009).

2. Novoselov K S A, Geim A K, Morozov S V, et al. "Two-dimensional gas of massless Dirac fermions in graphene[J]". *nature*, 438(7065): 197-200 (2005).

3. Horng J, Chen C F, Geng B, et al. "Drude conductivity of Dirac fermions in graphene[J]". *Physical Review B*, 83(16): 165113 (2011).

4. Liu M, Yin X, Ulin-Avila E, et al. "A graphene-based broadband optical modulator[J]". *Nature*, 474(7349): 64-67 (2011).

5. Ju L, Geng B, Horng J, et al. "Graphene plasmonics for tunable terahertz metamaterials[J]". *Nature nanotechnology*, 6(10): 630-634 (2011).

6. Yang K, Arezoomandan S, Sensale-Rodriguez B. "The linear and nonlinear THz properties of graphene[J]". *Terahertz Sci. Technol*, 6(4): 223-233 (2013).

7. Vakil A, Engheta N. "Transformation optics using graphene[J]". *Science*, 332(6035): 1291-1294 (2011).

8. Sanderson M, Ang Y S, Gong S, et al. "Optical bistability induced by nonlinear surface plasmon polaritons in graphene in terahertz regime[J]". *Applied Physics Letters*, 107(20): 203113 (2015).

9. Grigorenko A N, Polini M, Novoselov K S. "Graphene plasmonics[J]". *Nature photonics*, 6(11): 749-758 (2012).

10. Ryzhii M, Ryzhii V. "Injection and population inversion in electrically induced p–n junction in graphene with split gates[J]". *Japanese journal of applied physics*, 46(3L): L151 (2007).

11. Liu S, Zhang C, Hu M, et al. "Coherent and tunable terahertz radiation from graphene surface plasmon polaritons excited by an electron beam[J]". *Applied Physics Letters*, 104(20): 201104 (2014).

12. Tantiwanichapan K, Wang X, Swan A K, et al. "Graphene on nanoscale gratings for the generation of terahertz Smith-Purcell radiation[J]". *Applied Physics Letters*, 105(24): 241102 (2014).

13. Zhan T, Han D, Hu X, et al. "Tunable terahertz radiation from graphene induced by moving electrons[J]". *Physical Review B*, 89(24): 245434 (2014).

14. Zhao T, Sen Gong M H, Zhong R, et al. "Coherent and Tunable Terahertz Radiation from Graphene Surface Plasmon Polarirons Excited by Cyclotron Electron Beam[J]". *Scientific reports*, 5: 16059 (2015).

15. Gao W, Shi G, Jin Z, et al. "Excitation and active control of propagating surface plasmon polaritons in graphene[J]". *Nano letters*, 13(8): 3698-3702 (2013).

16. Bludov Y V, Ferreira A, Peres N M R, et al. "A primer on surface plasmon-polaritons in graphene[J]". *International Journal of Modern Physics B*, 27(10): 1341001 (2013).

17. Zhou W, Lee J, Nanda J, et al. "Atomically localized plasmon enhancement in monolayer graphene[J]". *Nature nanotechnology*, 7(3): 161-165 (2012).

18. Ochiai T. “Efficiency and Angular Distribution of Graphene-Plasmon Excitation by Electron Beam[J]”. *Journal of the Physical Society of Japan*, 83(5): 054705 (2014).

19. Garcıía de Abajo F J. “Multiple excitation of confined graphene plasmons by single free electrons[J]”. *ACS nano*, 7(12): 11409-11419 (2013).

20. Gong S, Zhao T, Sanderson M, et al. “Transformation of surface plasmon polaritons to radiation in graphene in terahertz regime[J]”. *Applied Physics Letters*, 106(22): 223107 (2015).

21. Gong S, Hu M, Zhong R, et al. “Electron beam excitation of surface plasmon polaritons[J]”. *Optics express*, 22(16): 19252-19261 (2014).